CHIN. PHYS. LETT. Vol. 38, No. 2 (2021) 026101

Structural and Electrical Properties of $Be_xZn_{1-x}O$ Alloys under High Pressure

Yanling Zhang(张艳玲), Xiaozhu Hao(郝晓竹), Yanping Huang(黄艳萍), Fubo Tian(田夫波)*, Da Li(李达), Youchun Wang(王友春), Hao Song(宋昊), and Defang Duan(段德芳)

State Key Laboratory of Superhard Materials, College of Physics, Jilin University, Changchun 130012, China

(Received 2 September 2020; accepted 18 November 2020; published online 27 January 2021)

We conduct extensive research into the structures of $Be_xZn_{1-x}O$ ternary alloys in a pressure range of 0–60 GPa, using the *ab initio* total energy evolutionary algorithm and total energy calculations, finding several metastable structures. Our pressure-composition phase diagram is constructed using the enthalpy results. In addition, we calculate the electronic structures of the $Be_xZn_{1-x}O$ structures and investigate the bandgap values at varying pressures and Be content. The calculated results show that the bandgap of the $Be_xZn_{1-x}O$ ternary alloys increases with an increase in Be content at the same pressure. Moreover, the bandgap of the $Be_xZn_{1-x}O$ ternary alloys increases with the increasing pressure with fixed Be content. At the same Be content, the formation enthalpy of the $Be_xZn_{1-x}O$ ternary alloys first decreases, then increases with the increasing pressure.

DOI: 10.1088/0256-307X/38/2/026101

In recent years, zinc oxide (ZnO), a kind of functional device material, has attracted much attention due to its excellent characteristics and great significance in the fields of optics, electricity, photoelectricity, piezoelectricity, and magnetism. ZnO is a Ⅱ–Ⅵ oxide semiconductor with a wide bandgap, large exciton binding energy, low dielectric constant, large photoelectric coupling rate, piezoelectric polarizations, and strong structural stability.[1–4] Therefore, ZnO has great potential applications in ultraviolet detectors, blue-ray ultraviolet light-emitting photoelectric devices, lasers, light-emitting diodes, gas-sensitive sensors, piezoelectric devices, photocatalysis, and solar cells.[5–11] Currently the research into ZnO falls into three main categories: finding an n-type semiconductor with good properties, obtaining a stable p-type conduction, and bandgap modulation of ZnO in order to extend the energy bandgap. In addition, ZnO can be used in quantum wells and super lattices.[12–18] In the last decade, it has been demonstrated that ZnO can form ternary compounds with MgO and CaO, which possess wider bandgaps.[19,20] $Mg_xZn_{1-x}O$ ternary alloys allow a modulation of the bandgap over a wide range, from 3.34 to 7.8 eV.[21] $Ca_xZn_{1-x}O$ ternary alloys are also candidates for promoting a wider bandgap because CaO is itself a compound with wide bandgap of 7.2 eV.[22] It has been suggested that the solubility of MgO and CaO in alloys is low due to lattice mismatch. However, both calculations and experiments confirm that their solubility depends strongly on external conditions, and can be considerably increased at high temperatures and high pressures.[23,24] Our previous studies have shown that $Mg_xZn_{1-x}O$ and $Ca_xZn_{1-x}O$ ternary alloys exhibit stable state structures at high pressures.[25,26] BeO and ZnO share the same hexagonal symmetry, and BeO is considered to be one of the best alternative materials for achieving wide bandgap modulation, presenting many advantages for technological applications.[27–29] In an experiment, BeZnO films were deposited using the hybrid beam deposition growth method, and the energy bandgap modulation range of the resulting $Be_xZn_{1-x}O$ ternary alloys varies from the ZnO bandgap (3.4 eV) to that of BeO (10.6 eV).[30] Owing to their superior characteristics, a great deal of attention has been devoted to $Be_xZn_{1-x}O$ ternary alloys, in terms of their synthetic growth in the experiments and the theoretical evaluation of their properties. Numerous theoretical and experimental works on $Be_xZn_{1-x}O$ ternary alloys are available.[31–34] Dong *et al.* investigated the structures and related properties of $Be_xZn_{1-x}O$ alloys at zero pressure,[35] and their structures were from the supercells of known ZnO or BeO structures by replacing atoms.

High pressure may induce phase transitions and has profound effects on the structures, as well as the physical and chemical properties of materials. As we all know, diamond is a metastable structure, which can be obtained from graphite under high pressure and high temperature. In addition, it can be quenched and preserved under ambient conditions. Previous studies have shown that pressure can cause great changes in molecules.[36,37] In this study, we investigate the struc-

Supported by the National Key Research and Development Program of China (Grant Nos. 2016YFB0201204, 2018YFA0703404, and 2017YFA0403704), the National Natural Science Foundation of China (Grant Nos. 11574109 and 91745203), and the Program for Changjiang Scholars and Innovative Research Team in Universities (Grant No. IRT_15R23).

*Corresponding author. Email: tianfb@jlu.edu.cn

© 2021 Chinese Physical Society and IOP Publishing Ltd

tures of different compositions of $Be_xZn_{1-x}O$ ternary alloys, at pressures ranging from 0 to 60 GPa, via first-principles calculations with local density approximation methods. We examine the structural and electronic properties of $Be_xZn_{1-x}O$ ternary alloys at different pressures and Be concentrations. In recent years, several studies have been conducted in relation to these compounds. However, systematic studies based on different ratios are still lacking. In this Letter, we use first-principles calculations to analyze the $Be_xZn_{1-x}O$ ternary alloys, with the aim of providing a comprehensive theoretical underpinning for future research.

The USPEX (Universal Structure Predictor: Evolutionary Xtallography) crystal structure prediction software package based on the genetic evolution algorithm was used to conduct a systematic structural search for $Be_xZn_{1-x}O$ ternary alloys in a pressure range 0–60 GPa.[38] First generation structures were randomly generated. The worst-energy structures (40%) were discarded, and the new generation evolved from the remaining structures. The best structures in each generation were carried forward to the next generation. We generally halted the runs after 60 generations, and all runs found the minimum enthalpy structures earlier. We searched for and predicted the crystal structures of $Be_xZn_{1-x}O$ ternary alloys at pressures of 0–60 GPa. The Vienna *ab initio* simulation package (VASP) based on the density functional theory (DFT)[39] was used to optimize the crystal structure and to determine its crystalline properties using the local density approximation (LDA).[40] To verify the bandgap results, we used the GPU version of PWmat code with the hybrid function of Heyd, Scuseria and Ernzerhof (HSE)[41] to calculate the bandgaps. The PWmat code has proven to be accurate and effective in calculations relating to semiconductor systems.[42,43] We determined the interaction between electrons and ions using the projector augmented plane wave method.[44] During structural optimization, the plane-wave basis set cutoff energy of the system 850 eV, and the Brillouin zone (BZ) integrals performed using a Monkhorst–Pack[45] sampling scheme with a k-point mesh resolution of $2\pi \times 0.03\,\text{Å}^{-1}$. The total energies were found to be well converged to within 1 meV/atom.[46] The phonon spectrum was determined using the supercell method via the PHONOPY program.[47]

In this work, we calculated the phase diagram and the formation enthalpy of $Be_xZn_{1-x}O$ ternary alloys in a pressure range from 0–60 GPa, using the density functional theory. Several predicted structures were observed at different pressures. These structures include $BeZn_4O_5$ ($P2_1$, $Pmn2_1$), $BeZn_3O_4$ ($Pmn2_1$-a, $Pmn2_1$-b), $BeZn_2O_3$ ($Cmc2_1$, $Pmma$), $BeZnO_2$ ($Pna2_1$, $Pca2_1$), Be_2ZnO_3 ($Cmc2_1$), Be_3ZnO_4 ($Pmn2_1$, $C2$), Be_5ZnO_6 ($P31m$), and $Be_2Zn_3O_5$ ($Cmc2_1$), as illustrated in Fig. 1. The formation enthalpies of all the $Be_xZn_{1-x}O$ structures were evaluated via fractional notation, and decomposed into BeO and ZnO as follows:

$$\Delta H(Be_xZn_{1-x}O) = H(Be_xZn_{1-x}O) - [xH(BeO) + (1-x)H(ZnO)],$$

where x is the concentration of the BeO, and H represents the enthalpy of the corresponding structure under a specific pressure. The calculated results are shown in Fig. 2. All the formation enthalpies of the structures we predicted are positive, indicating that these structures are metastable. The calculated results show that there are no stable state structures in the $Be_xZn_{1-x}O$ system at atmospheric or high pressure, although BeO and ZnO share a similar structure. This may be caused by the large difference between the Be and Zn atomic radii, or the lattice constants of BeO and ZnO.

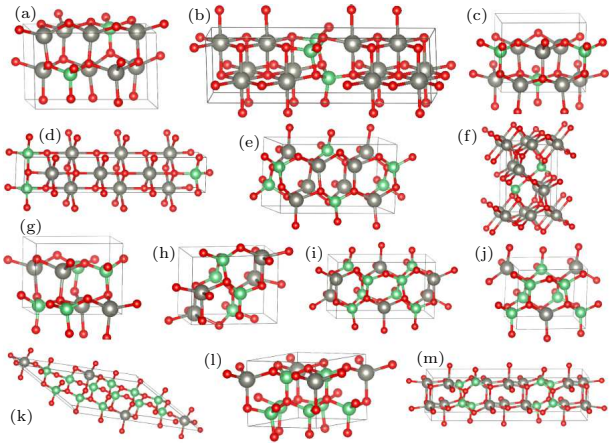

Fig. 1. Crystalline structures at different pressures for the predicted $BeZn_4O_5$, $BeZn_3O_4$, $BeZn_2O_3$, $BeZnO_2$, Be_2ZnO_3, Be_3ZnO_4, Be_5ZnO_6, and $Be_2Zn_3O_5$. The large gray, medium-sized green and small red spheres represent Zn, Be and O atoms, respectively.

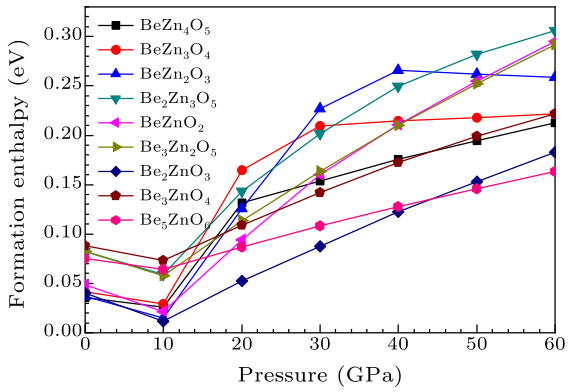

Fig. 2. Formation enthalpy of $Be_xZn_{1-x}O$ ternary alloys.

The Be_2ZnO_3, Be_5ZnO_6, and $Be_2Zn_3O_5$ are stable in the $Cmc2_1$, $P31m$, and $Cmc2_1$ structures, respectively, at pressures ranging from 0 to 60 GPa. While for $BeZn_4O_5$, $BeZn_3O_4$, $BeZn_2O_3$, $BeZnO_2$,

and Be_3ZnO_4, each of them has two structures, we therefore calculated the difference in enthalpy, and the results are shown in Fig. 3. From 0 to 16 GPa, $BeZn_4O_5$ is stable in the $P2_1$ structure, then transforms into a $Pmn2_1$ structure. For $BeZn_3O_4$, the two $Pmn2_1$ structures (referred to as $Pmn2_1$-a and $Pmn2_1$-b) are found to be most stable over pressure ranges of 0–26 and 26–60 GPa, respectively. $BeZn_2O_3$ is stable in $Cmc2_1$ symmetry at zero pressure, transforming into a $Pmma$ structure at 34 GPa. For $BeZnO_2$, $Pna2_1$ and $Pca2_1$ structures are found to be most stable in the pressure ranges of 0–29 and 29–60 GPa, respectively. The $Pmn2_1$ to $C2$ Be_3ZnO_4 transformation occurs at 46 GPa.

To further determine the stability of the structures, we calculated the phonon dispersion spectra at different pressures, with some of the results provided in Fig. 4. No imaginary phonon frequency was observed across the whole Brillouin zone (BZ), indicating that all the structures are dynamically stable in the pressure range under consideration. The calculated results mentioned above allowed us to construct a P–x phase diagram of $Be_xZn_{1-x}O$ ternary alloys (see Fig. 5).

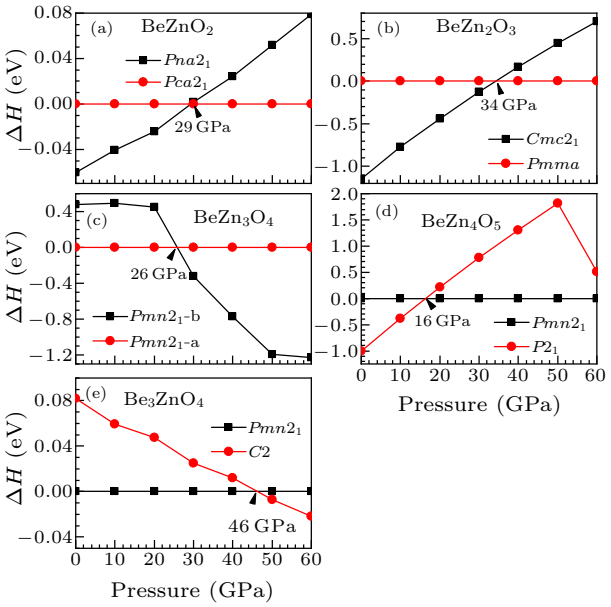

Fig. 3. Calculated enthalpies versus pressure.

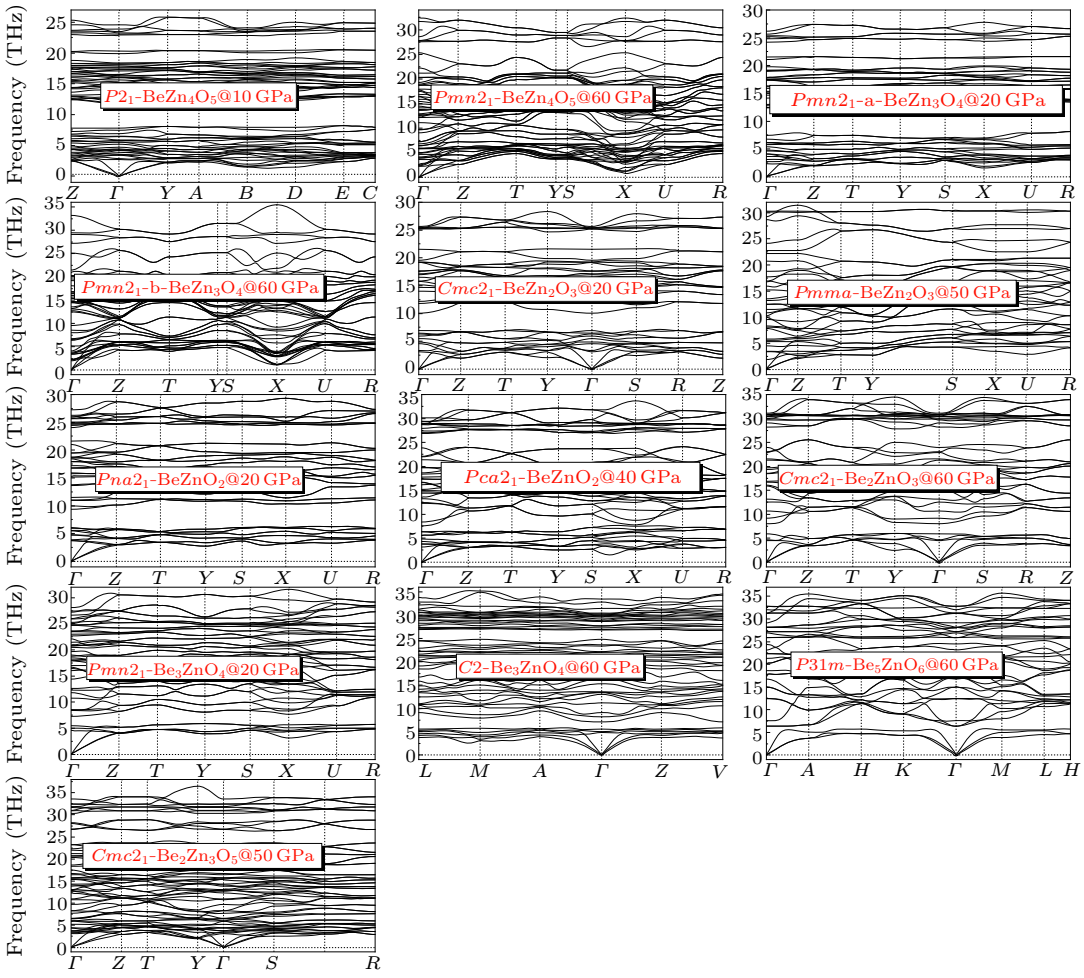

Fig. 4. Phonon dispersive curves for $BeZn_4O_5$, $BeZn_3O_4$, $BeZn_2O_3$, $BeZnO_2$, Be_2ZnO_3, Be_3ZnO_4, Be_5ZnO_6, and $Be_2Zn_3O_5$.

We then plot the change in energy bandgap with Be content using the local density approximation, as shown in Fig. 6. The bandgap variation between the various $Be_xZn_{1-x}O$ ternary alloys is approximately linear. Bandgap refers to the energy change between valence band maximum (VBM) and conduction band minimum (CBM), which is one of the most important parameters for measuring the photoelectric properties of semiconductors. Figure 6 shows that for the same Be content, the bandgap of the $Be_xZn_{1-x}O$ ternary alloys increases with the increasing pressure. We also observed that the bandgap of the $Be_xZn_{1-x}O$ ternary alloys increases when the Be content is increased at the same pressure. In addition, we calculated the bandgaps using the HSE functional for comparison, as shown in Fig. 6, which indicates that, although the LDA significantly underestimates the bandgap by about 2.5 eV, the variation trend in the LDA bandgaps with increasing Be content is consistent with that of the HSE method.

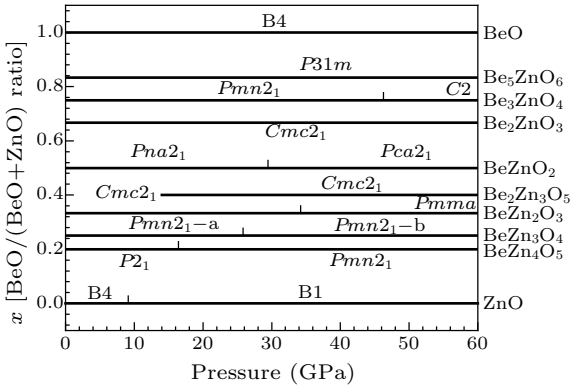

Fig. 5. Pressure-composition phase diagram of $Be_xZn_{1-x}O$ alloys.

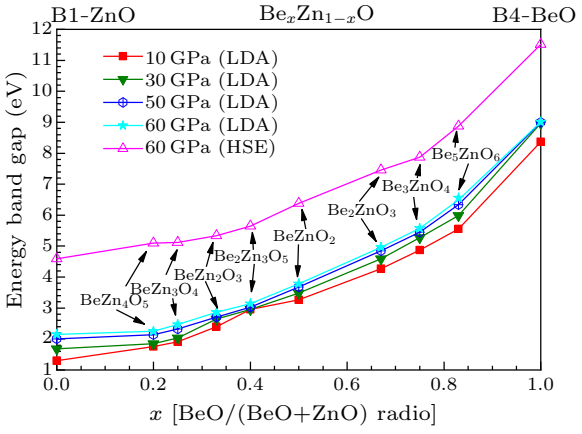

Fig. 6. The energy band-gap of $Be_xZn_{1-x}O$ alloys as a function of BeO concentration at different pressures, using LDA and HSE.

On the basis of the *ab initio* evolutionary algorithm, we successfully predicted several metastable structures of $Be_xZn_{1-x}O$ ternary alloys at pressures ranging from 0 to 60 GPa. These structures include $BeZn_4O_5$, $BeZn_3O_4$, $BeZn_2O_3$, $BeZnO_2$, Be_2ZnO_3, Be_3ZnO_4, Be_5ZnO_6, and $Be_2Zn_3O_5$. The calculated results show that the bandgap of the $Be_xZn_{1-x}O$ ternary alloys increases with an increase in Be content at the same pressure. Moreover, the bandgap of the $Be_xZn_{1-x}O$ ternary alloys increases with the increasing pressure with fixed Be content. At the same Be content, the formation enthalpy of the $Be_xZn_{1-x}O$ ternary alloys first decreases, then increases with the increasing pressure. Our results may be useful for band-structure engineering where $Be_xZn_{1-x}O$ ternary alloys are considered for use in optoelectronic devices and other applications.

Some of our calculations were performed at the High-Performance Computing Center (HPCC) of Jilin University.

References

[1] Rensmo H, Keis K, Henrik L, Sven A S, Solbrand A, Anders H and Sten-Eric L 1997 *J. Phys. Chem. B* **101** 2598
[2] Kumari L and Kar A K 2018 *AIP Conf. Proc.* **1953** 030158
[3] Zhang F C, Zhang Z Y and Zhang W H 2009 *Chin. Phys. B* **18** 2508
[4] Tonkoshkur A S and Ivanchenko A V 2019 *J. Adv. Dielectr.* **9** 1950023
[5] Li Z and Yu L B 2019 *Sol. Energy* **184** 315
[6] Hu P S, Wu C E and Chen G L 2018 *Materials* **11** 3
[7] Gedamu D, Paulowicz I, Lupan O, Wille S, Haidarschin G, Mishra Y K and Adelung R 2014 *Adv. Mater.* **26** 1541
[8] Wei M, Xu C X, Qin F F, Manohari A G, Lu J F and Zhu Q X 2017 *Chin. Phys. Lett.* **34** 078503
[9] Zhang Q, Li G Y, Liu X F, Qian F, Li Y, Sum T Z, Lieber C M and Xiong Q H 2014 *Nat. Commun.* **5** 4953
[10] Mahroug A, Amari R, Boukhari A, Deghfel B, Guerbous L and Selmi N 2018 *J. Nanoelectron. Optoelectron.* **13** 732
[11] Huang J D and Jiang J Y 2019 *RSC Adv.* **9** 29967
[12] Tsukazaki A, Ohtomo A, Onuma T, Ohtani M and Kawasaki M 2004 *Nat. Mater.* **4** 42
[13] Ganesh V, Yahia I S, Alfaify S and Shkir M 2017 *J. Phys. Chem. Solids* **100** 115
[14] Al-Hardan N H, Rashid M M M, Aziz A A and Ahmed N M 2019 *J. Mater. Sci.: Mater. Electron.* **30** 19639
[15] Zheng H, Chen Z, Zhu H, Tang Z and Shan X 2020 *Chin. Phys. B* **29** 097302
[16] Weston L, Cui X Y, Delley B and Stampfl C 2012 *Phys. Rev. B* **86** 205322
[17] Wang Y C, Tian F B, Li D, Duan D F, Xie H, Liu B B, Zhou Q and Cui T 2019 *J. Alloys Compd.* **788** 905
[18] Long D B, Li M K, Luo M H, Zhu J K, Yang H, Huang Z B, Ahuja R and He Y B 2017 *Mater. Res. Express* **4** 055901
[19] Maznichenko I V, Ernst A, Bouhassoune M, Henk J, Daene M, Lueders M, Bruno P, Herget W, Mertig I, Szotek Z and Temmerman W M 2009 *Phys. Rev. B* **80** 144101
[20] Shimada K, Takahashi N, Nakagawa Y, Hiramatsu T and Kato H 2013 *Phys. Rev. B* **88** 075203
[21] Wu C C, Wuu D S, Lin P R, Chen T N, Horng R H, Ou S L, Tu Y L, Wei C C and Feng Z C 2011 *Thin Solid Films* **519** 1966
[22] Richet P, Mao H K and Bell P M 1988 *J. Geophys. Res.* **93** 15279
[23] Solozhenko V L, Baranov A N and Tukevich A N 2006 *Solid State Commun.* **138** 534
[24] Sanati M, Hart G L W and Zunger A 2003 *Phys. Rev. B* **68** 155210

[25] Tian F, Duan D, Li D, Chen C, Sha X, Zhao Z and Cui T 2014 *Sci. Rep.* **4** 5759
[26] Sha X J, Tian F B, Li D, Duan D F, Chu B H, Liu Y X, Liu B B and Cui T 2015 *Sci. Rep.* **5** 11003
[27] Jaffe J E, Synder J A, Lin Z and Hess A C 2000 *Phys. Rev. B* **62** 1660
[28] Mori Y, Niiya N, Ukegawa K, Mizuno T, Takarabe K and Ruoff A L 2004 *Phys. Status Solidi B* **241** 3198
[29] Duan Y, Shi H, Qin L 2008 *Phys. Lett. A* **372** 2930
[30] Ryu Y R, Lee T S, Lubguban J A, Corman A B and White H W 2006 *Appl. Phys. Lett.* **88** 052103
[31] Lakel S, Elhamra F, Almi K and Meradji H 2015 *Mater. Sci. Semicond. Process.* **40** 803
[32] Li M K, Luo M H, Zhu J K, Long D B, Miao L S and He Y B 2017 *J. Appl. Phys.* **121** 205101
[33] Elhamra F, Lakel S, Ibrir M, Almi K and Meradji H 2015 *Mod. Phys. Lett. B* **29** 1550140
[34] Elhamra F, Lakel S and Meradji H 2016 *Optik* **127** 1754
[35] Dong L and Alpay S P 2011 *Phys. Rev. B* **84** 035315
[36] Paul F and M 2002 *Nat. Mater.* **1** 19
[37] Duan D F, Huang X L, Tian F B, Yu H Y, Liu Y X, Ma Y M, Liu B B and Cui T 2015 *Phys. Rev. B* **91** 180502
[38] Oganov A R, Lyakhov A O and Valle M 2011 *Acc. Chem. Res.* **44** 227
[39] Kresse G and Furthmüller J 1996 *Phys. Rev. B* **54** 11169
[40] Kawatani T, Shimizu H 1998 *Proceedings. Fourteenth International Conference on Pattern Recognition (Cat. No. 98EX170)*, Brisbane, Queensland, Australia, 20 August 1998, vol 2 pp 1301–1305
[41] Heyd J, Scuseria G E and Ernzerhof M 2003 *J. Chem. Phys.* **118** 8207
[42] Jia W, Cao Z, Wang L, Fu J, Chi X, Gao W and Wang L W 2013 *Comput. Phys. Commun.* **184** 9
[43] Jia W, Fu J, Cao Z, Wang L, Chi X, Gao W and Wang L W 2013 *J. Comput. Phys.* **251** 102
[44] Blöchl P E 1994 *Phys. Rev. B* **50** 17953
[45] Monkhorst H J and Pack J D 1976 *Phys. Rev. B* **13** 5188
[46] Chadi D J 1977 *Phys. Rev. B* **16** 1746
[47] Togo A, Oba F and Tanaka I 2008 *Phys. Rev. B* **78** 134106